

Ductile Fracture Analysis of IPIRG Cracked Pipe Experiments Using Strain Energy Density Criterion

Jing-Jong SHIE, Kuen TING
Institute of Nuclear Energy Research, Lung-Tan, China

1 INTRODUCTION

The application of elastic-plastic fracture mechanics techniques to structural integrity assessments of nuclear piping is important to quantify the margin of safety. Several investigations have been devoted to focus on J-integral approach to predict conditions for initiation, stable growth and the onset of instability of cracks in nuclear power plant piping (Zahoor 1988). However, this approach suffers serious limitations in prediction of the slow stable crack growth behavior prior to the onset of fast fracture. In a series of publications the strain energy density criterion was used to study the problem of ductile fracture. The purpose of this work is to apply the strain energy density criterion to predict the crack initiation and growth for the circumferential through-wall cracked piping.

Based on the Sih's theory (Sih and Madenci 1983), a stable crack growth takes place when material elements ahead of the crack tip absorb a critical amount of strain energy density, $(dW/dV)_c$. This critical value can be calculated from the area underneath the true stress-true strain curve. The calculations of the strain energy density field can be carried out by the finite element program "ABAQUS" version 4.8 (Hibbitt 1989).

The incremental procedure considering the finite deformation and elastic-plastic behavior associated with von-Mises yield criterion, isotropic hardening and Prandtl-Reuss flow rule is employed.

To demonstrate the accuracy and the validity of the failure criterion proposed herein, the degraded piping experiment 4131-5 conducted by Battelle Laboratory is analyzed. Results of the critical loads of crack initiation and growth are compared with the experimental data. Good correlations are drawn in this work.

2 STRAIN ENERGY DENSITY CRITERION

Based on Sih's theory (Sih 1981), the strain energy criterion has been employed to predict the onset of the crack growth. This concept is applied to obtain the stationary

values of the strain energy density function along the circular core region with radius r_0 , that surrounds the crack tip. The strain energy density function dW/dV is defined as

$$\frac{dW}{dV} = \int_0^{\epsilon_{ij}} \sigma_{ij} d\epsilon_{ij} \quad (1)$$

in which σ_{ij} and ϵ_{ij} are stress and strain components, respectively. The hypotheses on fracture initiation can be stated as follows:

- (1) The location of fracture initiation is assumed to coincide with the maximum of minimum strain energy density function $(dW/dV)_{min}^{max}$.
- (2) Failure by fracture is assumed to occur when $(dW/dV)_{min}^{max}$ reaches its critical value $(dW/dV)_c$.

Referring to the uniaxial true stress-true strain curve for a typical engineering material in Fig.1, the critical strain energy density function corresponding to failure, $(dW/dV)_c$ is the area OABB' and can be expressed as

$$\left(\frac{dW}{dV}\right)_c = \int_0^{\epsilon_u} \sigma d\epsilon \quad (2)$$

where ϵ_u is the ultimate strain, σ is true stress and ϵ is true strain.

3 BRIEF DESCRIPTION OF DEGRADED PIPING EXPERIMENT 4131-5

The objective of experiment 4131-5 was to collect data on a 6-inch (152mm) nominal diameter Schedule 120 SA-376 TYPE 304 stainless steel pipe with an idealized circumferential through-wall crack subjected to four-point bending until failure (IPIRG-DRB 1.1.1.12 1986). This experiment was performed at quasi-static loading type and at the temperature 288 °C. The crack was an idealized through-wall crack with a circumferential length of 38.8 percent of the pipe's circumference. The true stress-true strain curve of pipe material (identification DP2-A23) is shown in Fig.2. The critical strain energy density is 149.6 MJ/m³ which can be computed from Fig.2. The initiation load for two crack-tips were 60.1 kN and 57.0 kN, respectively. Maximum load achieved during the test was 74.2 kN.

4 FINITE ELEMENT ANALYSIS

The computations have been performed by the finite element code "ABAQUS" version 4.8. Due to symmetric geometry and applied loading, only a quarter portion of the pipe is required for analyzing. The three dimensional finite element model is shown in Fig.3. Two layers of the elements are arranged in the pipe thickness. Total numbers of the 3D 20-nodes isoparametric elements and that of nodes of this model are 286

and 1996, respectively. This analysis is approached by the generation mode, i.e., basic controlled load-line displacements together with measured crack growth increments are input to ABAQUS, as shown in Fig. 4. Crack extension is simulated by the nodal releasing technique.

5 RESULTS AND DISCUSSIONS

Performing the finite element studies of through-wall cracked pipe, the distributions of strain energy density function along the distance normal to the crack front at the applied load-line displacement $\delta=33.6$ and 39.6 mm are shown in Fig. 5. The strain energy density curve of $\delta=39.6$ mm reaches the critical value $(dW/dV)_c$ at the crack growth increment $\Delta a=0.295$ mm. Based on the previous experiences (Ting 1991, Sih 1984), the radius of core region r_c is assumed as 0.127 mm in this work. The crack growth increment $\Delta a=0.295$ mm is out of core region. Then the crack initiation takes place at $\delta=39.6$ mm as expected the experimental data. Fig. 6 illustrates the crack growth increments for various load steps. The applied load-line displacement δ versus the crack length Δa can thus be plotted in Fig. 4. Good correlations between the computed results based on the strain energy density criterion and the experimental data can be drawn. Finally, the relationship between the applied load P and load-line displacement δ is displayed in Fig. 7. There exists some difference between the calculated results and experimental data after the crack initiation.

6 CONCLUSION

A general method for the prediction of the crack initiation and growth of three dimensional ductile fracture problems is presented herein. Only the true stress-true strain curve is necessary to study the fracture behaviors. Good results can be found in this work. For evaluating the acceptability of the strain energy density criterion, the further analysis of IPIRG experiments will be studied in future.

REFERENCES

- Zahoor A. (1988). Ductile fracture mechanics methodology for complex cracks in nuclear piping, Nuclear Engineering and Design, Vol.106, pp.243-256.
- Sih, G.C. and Madenci, E. (1983). Fracture initiation under gross yielding: Strain energy density criterion, Engineering Fracture Mechanics, Vol.18, pp.667-677.
- Sih, G.C. and Madenci, E. (1983). Crack growth resistance characterized by the strain energy density function, Engineering Fracture Mechanics, Vol.18, pp.1159-1171.

Hibbitt, Karlson and Sorensen (1989) ABAQUS Users Manual, H.K.S. INC.

Sih, G.C. (1981). Experimental fracture mechanics: Strain energy density criterion, In Mechanics of fracture, Vol. VII: Experimental evaluation of stress concentration and intensity factors, (edit by G.C. Sih), pp XVIII-LVI.

IPIRG (1988). International piping integrity research program, Data Record Book 1.1.1.12, (edit by Battelle Laboratory)

Ting, K. and Shie, J.J. (1991). The application of strain energy density criterion to crack initiation in mixed mode ductile fracture problem, SMiRT-11

Sih, G.C. (1984). "The strain energy density criterion" in "Problems of mixed mode crack propagation" (edit by Gdoutos, E.E.) Martinus, Nijhoff Publishers, pp.1-10.

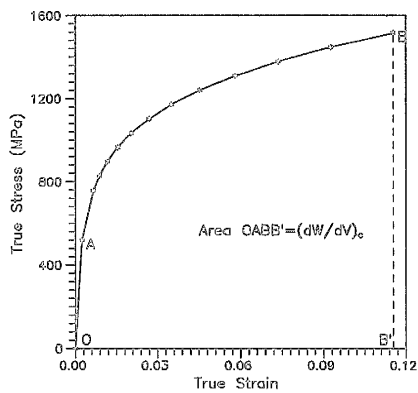


Fig. 1 True stress-true strain curve of an elastic-plastic material

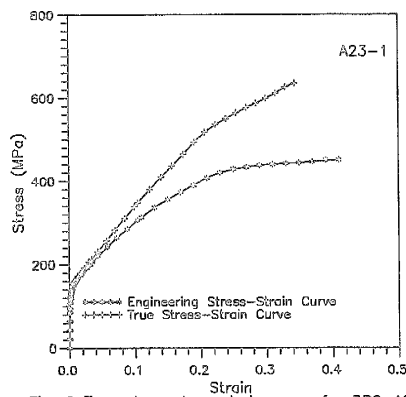


Fig. 2 True stress-true strain curve for DP2-A23

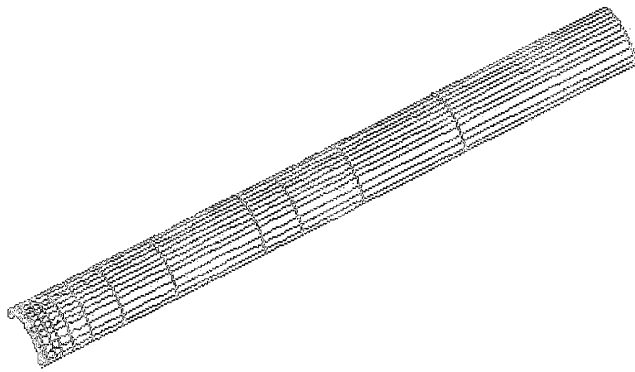


Fig. 3.a Finite element model

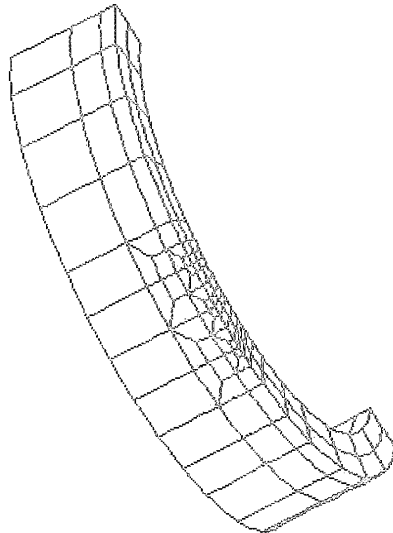


Fig. 3.b Local grid pattern of cracked pipe

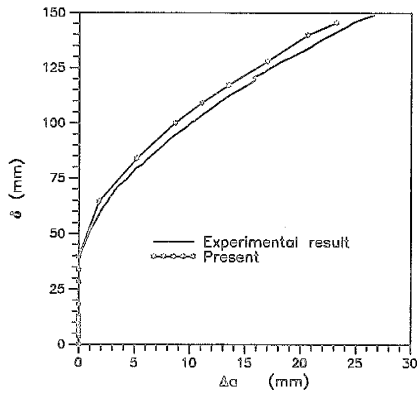
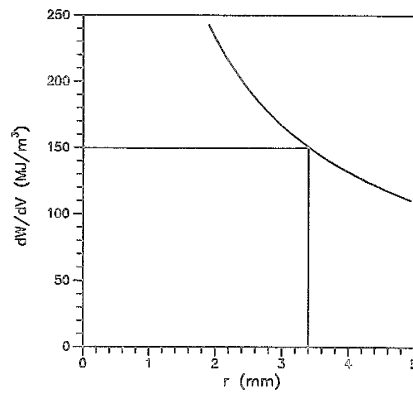


Fig. 4 Applied load line displacement versus crack length for experiment 4131-5



(a) $\delta=84.6$ mm

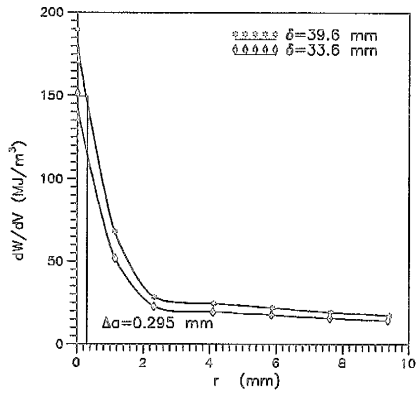
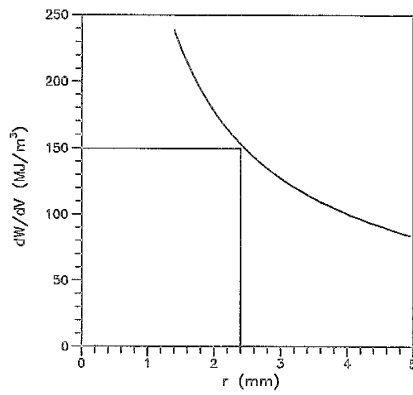


Fig. 5 The prediction of the critical value at the crack initiation



(b) $\delta=117.3$ mm

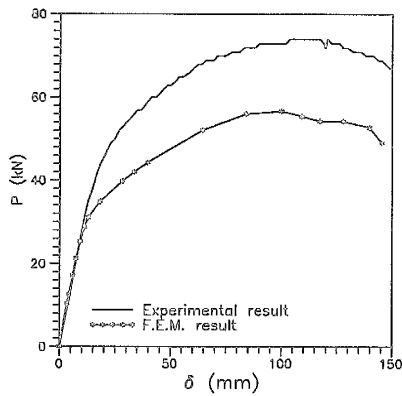
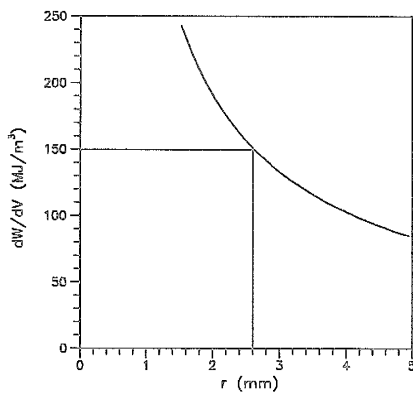


Fig. 7 Applied load versus load-line displacement for experiment 4131-5



(c) $\delta=146.2$ mm

Fig. 6 The prediction of the crack growth increments for various applied load